DOUBLE DEGENERATE MERGERS AS PROGENITORS OF HIGH-FIELD MAGNETIC WHITE DWARFS

Enrique García-Berro[1,2], Pablo Lorén-Aguilar[1,2], Gabriela Aznar-Siguán[1,2], Santiago Torres[1,2], Judit Camacho[1,2],
Leandro G. Althaus[3,4], Alejandro H. Córsico[3,4], Baybars Külebi[2,5], and Jordi Isern[2,5]

[1] Departament de Física Aplicada, Universitat Politècnica de Catalunya, c/Esteve Terrades, 5, 08860 Castelldefels, Spain; garcia@fa.upc.edu
[2] Institute for Space Studies of Catalonia, c/Gran Capità 2–4, Edif. Nexus 104, 08034 Barcelona, Spain
[3] Facultad de Ciencias Astronómicas y Geofísicas, Universidad Nacional de La Plata, Paseo del Bosque s/n, (1900) La Plata, Argentina
[4] Instituto de Astrofísica La Plata, IALP (CCT La Plata), CONICET, Argentina
[5] Institut de Ciències de l'Espai (CSIC), Facultat de Ciències, Campus UAB, Torre C5-parell, 08193 Bellaterra, Spain

ABSTRACT

High-field magnetic white dwarfs have been long suspected to be the result of stellar mergers. However, the nature of the coalescing stars and the precise mechanism that produces the magnetic field are still unknown. Here, we show that the hot, convective, differentially rotating corona present in the outer layers of the remnant of the merger of two degenerate cores can produce magnetic fields of the required strength that do not decay for long timescales. Using a state-of-the-art Monte Carlo simulator, we also show that the expected number of high-field magnetic white dwarfs produced in this way is consistent with that found in the solar neighborhood.

Key words: binaries: general – stars: evolution – stars: interiors – stars: magnetic field – stars: rotation – white dwarfs

1. INTRODUCTION

The merger of two white dwarfs has received considerable interest during the last several years because it is thought to be at the origin of several interesting astrophysical phenomena. In particular, the coalescence of two white dwarfs is one of the possible scenarios—the so-called double degenerate scenario—to account for Type Ia supernova outbursts (Webbink 1984; Iben & Tutukov 1984). Moreover, it is also thought that the merger of two degenerate cores could lead to the formation of magnetars (King et al. 2001). Also, three hot and massive white dwarf members of the Galactic halo could be the result of the coalescence of a double white dwarf binary system (Schmidt et al. 1992; Segretain et al. 1997). Additionally, hydrogen-deficient carbon and R Corona Borealis stars (Izzard et al. 2007; Clayton et al. 2007; Longland et al. 2011) are thought to be the consequence of the merging of two white dwarfs. Also, the large metal abundances found around some hydrogen-rich white dwarfs with dusty disks around them could also be explained by the merger of a carbon–oxygen and a helium white dwarf (García-Berro et al. 2007). Last, but not least, the phase previous to the coalescence of a double white dwarf close binary system has been shown to be a powerful source of gravitational waves that may eventually be detectable by *LISA* (Lorén-Aguilar et al. 2005). Here, we show that the merger of two degenerate cores can also explain the presence of very high magnetic fields in some white dwarfs—a result previously anticipated by Wickramasinghe & Ferrario (2000) but not yet quantitatively proved.

High-field magnetic white dwarfs have magnetic fields in excess of 10^6 G and up to 10^9 G (Schmidt et al. 2003). Surprisingly, very few belong to a noninteracting binary system (Kawka et al. 2007); moreover, they are more massive than the average for field white dwarfs (Silvestri et al. 2007). One possibility is that these white dwarfs descend from single stars, so the magnetic field is a fossil of previous evolution (Angel et al. 1981). However, this scenario cannot explain why these stars are massive or why they are not found in noninteracting binary systems. Recently, it has been suggested (Tout et al. 2008;

Nordhaus et al. 2011) that strong magnetic fields are produced during a common envelope episode in a close binary system in which one of the components is degenerate. During this phase, spiral-in of the secondary induces differential rotation in the extended convective envelope, resulting in a stellar dynamo that produces the magnetic field. However, the magnetic field produced in this way does not penetrate into the white dwarf, and it decays rapidly when the common envelope is ejected (Potter & Tout 2010).

In this paper, we show that the hot, differentially rotating, convective corona resulting from the merger of two degenerate cores produces strong magnetic fields that are confined to the outer layers of the resulting remnant and do not decay for very long timescales. The paper is organized as follows. In Section 2, we explain the precise mechanism that produces the required magnetic fields, and we show that these fields are confined the outer layers of the remnant of the coalescence and do not decay for very long timescales. Section 3 is devoted to analyzing whether our model can account for the number of high-field magnetic white dwarfs in the solar neighborhood. In Section 4, we summarize our findings and present our conclusions.

2. STELLAR DYNAMO

The merger of two degenerate cores is the final destiny of the evolution of a sizable fraction of binary systems. Three-dimensional simulations of the merger process (Guerrero et al. 2004; Yoon et al. 2007; Lorén-Aguilar et al. 2009) indicate that the remnant of the coalescence of two white dwarfs consists of a central white dwarf, which contains all the mass of the primary. On top of it is a hot corona, which is made up of approximately half of the mass of the disrupted secondary. Finally, surrounding this compact remnant, a rapidly rotating Keplerian disk is formed, containing nearly all the mass of the secondary that has not been incorporated into the hot corona. According to these calculations, little mass ($\sim 10^{-3}\,M_\odot$) is ejected from the system during the merger. The structure of the remnant of the coalescence is illustrated in Figure 1.

The existing simulations show that the temperature gradient in the hot corona is high; consequently, the corona is convective.
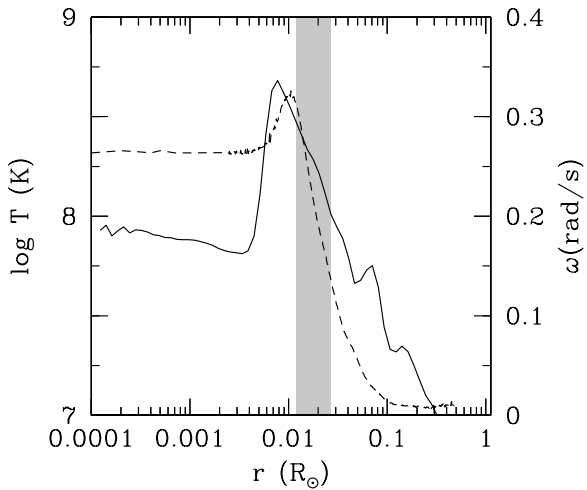
Figure 1. Dynamo configuration in a white dwarf merger. Temperature (solid line, left scale) and rotational velocity (dashed line, right scale) profiles of the final remnant of a white dwarf merger as a function of radius are shown for the case of a binary system composed of two stars of 0.6 and 0.8 $M_{\odot}$. In our simulations, approximately half of the mass of the disrupted secondary ($\sim 0.3\, M_{\odot}$) is accreted onto the primary, while the rest of the mass forms the Keplerian disk, which extends up to $\sim 0.3\, R_{\odot}$. The temperature of the central white dwarf depends on the initial temperature of the coalescing white dwarfs (Yoon et al. 2007; Lorén-Aguilar et al. 2009). However, the temperature of the hot corona is remarkably similar in all the simulations, $T \approx 8.7 \times 10^8$ K. The central spinning white dwarf rotates as a rigid body with a rotational velocity $\omega \sim 0.26$ s^{-1}, and the corona rotates differentially, with a peak rotation rate $\omega \sim 0.33$ s^{-1}. These velocities arise from energy and angular momentum conservation. Since little mass is ejected from the system, the orbital angular momentum of the binary system is invested in spinning up the remnant, while the available energy is primarily invested in heating the corona. The location of the convective region is displayed by the shaded area.

We computed the boundaries of the convective region using the Schwarzschild criterion, and we found that the inner and outer edges of the convective region are located at radii $R \approx 0.012\, R_{\odot}$ and $R \approx 0.026\, R_{\odot}$, respectively, and that the total mass inside this region is $\sim 0.24\, M_{\odot}$ (see Figure 1). Moreover, this region rotates differentially and is prone to magnetorotational instability. Assuming energy equipartition, the resulting $\alpha\omega$ dynamo produces a magnetic field $B^2/8\pi \approx \rho(\omega R)^2/2$. For the typical values found in the simulations of Lorén-Aguilar et al. (2009), the magnetic field amounts to $B \sim 3.2 \times 10^{10}$ G. Thus, the energy available in the convective corona is sufficiently large to produce strong magnetic fields. We note that, even in the case in which only 0.1% of the total energy of the convective shell is invested in magnetic energy, the fields produced in this way are on the order of 10^7 G, a value typical of high-field magnetic white dwarfs. We also note that there are very few white dwarfs with magnetic fields larger than 10^9 G, and, when these fields are observed, these are confined to spots on their surfaces.

For this mechanism to efficiently produce the observed magnetic fields, the dynamo must work for several convective turnovers before the energy of the hot corona is radiated away. The temperature of the corona is so high that is preferentially cooled by neutrino emission. The neutrino luminosity of the corona is $L_\nu \sim 4.0 \times 10^2\, L_{\odot}$, while the total thermal energy of the nondegenerate material in the corona is $U \sim 8.8 \times 10^{48}$ erg. Hence, the convective shell lasts for $\tau_{\mathrm{hot}} \sim 1.8 \times 10^5$ yr. The convective turnover timescale is $\tau_{\mathrm{conv}} \approx H_P/v_{\mathrm{conv}}$, where $H_P \approx 2.7 \times 10^8$ cm is the pressure scale height and $v_{\mathrm{conv}} \approx 8.0 \times 10^7$ cm s^{-1} is the convective velocity. Thus, $\tau_{\mathrm{conv}} \sim 3.3$ s, and, during the lifetime of the hot corona, the number of convective cycles is sufficiently large. Consequently, the $\alpha\omega$ mechanism

can produce a strong magnetic field. We also note that, if the duration of the convective shell is substantially smaller than what is estimated here, large magnetic fields can still be produced. Specifically, even assuming durations 10^3 times smaller than what was previously estimated, the number of convective cycles would still be enough to produce magnetic fields comparable with those observationally found in high-field magnetic white dwarfs. Thus, we conclude that the stellar dynamos produced in the aftermath of the merger of two degenerate cores can produce magnetic fields on the order of 10^7 G. From now on, we adopt this value (typical of high-field magnetic white dwarfs) as a fiducial value for the remaining calculations.

Once the magnetic field is established, we need to know if it can diffuse outward to the surrounding disk or inward to the degenerate primary. To this end, we solved the diffusion equation (Jackson 1998; Wendell et al. 1987):

$$\frac{\partial \vec{B}}{\partial t} = -\vec{\nabla} \times \left(\frac{c^2}{4\pi\sigma} \vec{\nabla} \times \vec{B} - \vec{v} \times \vec{B} \right), \qquad (1)$$

where σ is the magnetic conductivity, for which we used the most up-to-date prescription (Cassisi et al. 2007), while the rest of the symbols have their usual meaning. We first integrated the diffusion equation for the surrounding disk using cylindrical coordinates, adopting the velocity field, density, and temperature profiles resulting from our smoothed particle hydrodynamic (SPH) simulations (Lorén-Aguilar et al. 2009). The initial condition adopted here is $\vec{B}(0) = \vec{0}$, while we also imposed the boundary condition $\partial \vec{B}/\partial t = 0$ at the outer edge of the disk. We used a Crank–Nicolson integration scheme with variable coefficients (Dautray & Lions 2000), which turned out to be stable. We found that the timescale for diffusion of the magnetic field across the disk is $\tau_{\mathrm{disk}} \sim 2.0 \times 10^{11}$ yr. We did the same calculation, this time using spherical coordinates, to estimate the penetration of the magnetic field in the dense, degenerate primary. The use of spherical coordinates is perfectly justified because the departures of the compact primary from sphericity are very small. For this calculation, we followed the procedure outlined in Wendell et al. (1987). In this case, the electrical conductivity is totally dominated by degenerate electrons, and it depends on the adopted temperature of the isothermal white dwarf. If a temperature $T \approx 7.6 \times 10^7$ K is taken (Lorén-Aguilar et al. 2009), the diffusion timescale turns out to be $\tau_{\mathrm{WD}} \sim 4.3 \times 10^9$ yr. Since this timescale depends on the adopted initial temperature, we computed, using an up-to-date stellar evolutionary code (Renedo et al. 2010), a cooling sequence for a white dwarf of the mass, $1.1\, M_{\odot}$, and the chemical composition of the remnant, a carbon–oxygen core. The time to cool from 7.6×10^7 K to a value typical of field white dwarfs (say 3.0×10^6 K) is very short, $\tau_{\mathrm{cool}} \sim 3.0 \times 10^7$ yr. Hence, we can safely assume that, as the white dwarf cools, the rapid increase of the electrical conductivity does not allow the magnetic field to penetrate in the degenerate core of the primary, remaining confined to the surface layers.

Our model naturally predicts that the masses of high-field magnetic white dwarfs should be larger than average and that they should be observed as single white dwarfs, as observationally found—see, for instance, Valyavin & Fabrika (1999). However, high-field magnetic white dwarfs are generally found to be slow rotators (Wickramasinghe & Ferrario 2000). This apparent contradiction of the model can be easily solved. If the rotation and magnetic axes are misaligned, magnetodipole radiation rapidly spins down the white dwarf—see, however,

Timokhin ([2006](#)) and Spitkovsky ([2006](#)), where the time evolution of magnetospheres for axisymmetric and oblique rotators is described in detail. When both axes are misaligned, the evolution of the rotational velocity (Benacquista et al. [2003](#)) is

$$\dot{\omega} = -\frac{2\mu^2\omega^3}{3Ic^3}\sin^2\alpha, \qquad (2)$$

where I is the moment of inertia of the white dwarf, α is the angle between the magnetic and rotation axes, and $\mu = B R_{\mathrm{WD}}^3$. Thus, the spin-down timescale is simply $\tau_{\mathrm{MDR}} = \omega/2\dot{\omega}$. Adopting the values resulting from our SPH simulations (Lorén-Aguilar et al. [2009](#)), we obtain $\tau_{\mathrm{MDR}} \sim 2.4 \times 10^8/\sin^2\alpha$ yr for a field strength of $B = 10^7$ G. Hence, if both axes are perfectly aligned, the remnant of the coalescence will be a high-field, rapidly rotating magnetic white dwarf. By contrast, if both axes are nearly perpendicular, magnetodipole radiation efficiently brakes the remnant. Consequently, the very young, hot, ultramassive, slowly rotating magnetic white dwarfs 1RXS J0823.6−2525 and PG 1658+441, which have fields $\sim 3.5 \times 10^6$ G, can be accommodated in our model. For instance, PG 1658+441 has an effective temperature of $T_{\mathrm{eff}} \sim 30,000$ K and a mass of $M \sim 1.3\,M_\odot$ (Dupuis et al. [2003](#)), which corresponds to a cooling age of $\sim 3.7 \times 10^8$ yr, while the time needed to brake the white dwarf equals $\sim 8.4 \times 10^7$ yr if $\sin\alpha = 1$ is adopted. Thus, our model can account for the slow rotation rate of PG 1658+441, provided that the rotation and magnetic axes are misaligned. We also note at this point that, given the small radii—or, equivalently, the small radiating surfaces—of massive white dwarfs, their cooling ages markedly increase for effective temperatures smaller than $\log T_{\mathrm{eff}} \lesssim 4.7$.

On the other hand, rapidly rotating magnetic white dwarfs—of which an example is RE J 0317−853, a very massive ($\sim 1.3\,M_\odot$) white dwarf belonging to a wide binary system (Külebi et al. [2010](#))—could be the result of nearly equal-mass mergers in which both axes are aligned. In this case, no Keplerian disk is formed, so these white dwarfs will not show infrared excesses. If, by contrast, the masses of the coalescing white dwarfs are different, the axes are not aligned, and the disk can survive for a long-enough time, a second-generation planetary system could be eventually formed (García-Berro et al. [2007](#)) and tidal disruption and accretion of minor planets may contaminate the atmosphere of the white dwarf, resulting in magnetic DAZ or DAZd white dwarfs possibly showing infrared excesses. Examples of such white dwarfs are NLTT 10480 (Kawka & Vennes [2011](#)) and G77−50 (Farihi et al. [2011](#)), for which a satisfactory explanation of their origin is still lacking.

The geometry of the surface magnetic fields of white dwarfs has been investigated over the years using spectropolarimetric observations. The available wealth of observations shows that, in almost all cases, magnetic white dwarfs have fields strongly deviating from a dipolar structure. In particular, it appears that, in most cases, the geometry of the surface magnetic field corresponds to quadrupolar or higher multipoles—e.g., PG 1031+234 (Schmidt et al. [1986](#)), REJ 0317−855 (Ferrario et al. [1997](#)), HE 0241−0155 (Reimers et al. [2004](#)), HE 1045−0908 (Euchner et al. [2005](#)), or PG 1015+014 (Euchner et al. [2006](#)). This means that the toroidal component of the magnetic field must be stable and that a poloidal component should also be present. Our mechanism can also qualitatively reproduce these observations. Indeed, in the $\alpha\omega$ mechanism, convection is responsible for the generation of poloidal fields, whereas rotation is responsible for the generation of toroidal fields. Specifically, the energy available to generate the poloidal field component is

$\rho v_{\mathrm{conv}}^2/2 \sim 4.0 \times 10^{20}$ erg, which is $\sim 10\%$ of the energy available to build the toroidal component, $\rho(\omega R)^2/2 \sim 5.5 \times 10^{21}$ erg. Thus, we expect that the magnetic field generated by the fast-rotating convective shell will have both toroidal and poloidal field components. Moreover, it is well known that purely toroidal fields are unstable due to Tayler ([1973](#)) instability. However, the existence of a small poloidal component is a sufficient condition for stability. Actually, recent numerical studies (Braithwaite [2009](#)) show that the energy stored in the poloidal field component can be as high as 80% of the total magnetic energy, and even poloidal components 10^{-6} times smaller than the toroidal one are enough to warrant stability. Thus, toroidal fields generated by the rotating, convective shell produced in the merger of two double degenerates are stable; moreover, we expect that the magnetic fields generated in this way will have a complex geometry, which is in agreement with observations.

3. MAGNETIC WHITE DWARFS IN THE SOLAR NEIGHBORHOOD

To assess whether our scenario can reproduce the observed number of high-field magnetic white dwarfs, we have expanded an existing, state-of-the-art Monte Carlo code (García-Berro et al. [1999](#), [2004](#); Torres et al. [2002](#)) designed to study the Galactic populations of single white dwarfs to deal with those from double degenerates. In our simulations, we assumed that 50% of stars belong to binaries, and we normalized them to the local disk density of stars (Holmberg & Flynn [2000](#)). The initial primary masses were obtained using a standard initial mass function (Kroupa et al. [1993](#)) and the initial mass ratios were obtained according to a flat distribution. Also, a constant star formation rate and a disk age of 10^{10} yr were adopted. Orbital separations and eccentricities were randomly drawn according to a logarithmic probability distribution (Nelemans et al. [2001](#)) and to a thermal distribution (Heggie [1975](#)), respectively. For each of the components of the binary, analytical fits to detailed stellar evolutionary tracks were used (Hurley et al. [2000](#)), which provide full coverage from the main sequence until advance stages of evolution. For the white dwarf stage, the most recent cooling tracks of Renedo et al. ([2010](#)) were employed. The orbital evolution of each binary was computed by taking into account circularization and synchronization (Hurley et al. [2002](#)). We also considered mass losses through stellar winds. Specifically, we assumed that the evolution during the main sequence is conservative; only after it did we include stellar winds. The adopted mass-loss rate is that of Kudritzki & Reimers ([1978](#)) except on the asymptotic giant branch, for which the rate of Vassiliadis & Wood ([1993](#)) was used. Angular momentum losses due to magnetic braking and gravitational radiation were also included (Schreiber & Gänsicke [2003](#); Zorotovic et al. [2010](#)). The Roche lobe radius was computed using the most commonly used approximation (Eggleton [1983](#)), and during the overflow episodes both rejuvenation and ageing were taken into account (Hurley et al. [2002](#)). For the common envelope phase, we considered standard prescriptions for the common envelope efficiency and for the fraction of gravitational binding energy of the donor available to eject the envelope—see, e.g., Dewi & Tauris ([2000](#)). Specifically, we adopted $\alpha_{\mathrm{CE}} = 0.25$ and a variable value for the binding energy parameter λ (Zorotovic et al. [2010](#)). Using all these ingredients, we found that the fraction of merged double degenerate cores in the solar neighborhood is $\sim 2.9\%$ of the total synthetic population. This number includes not only white dwarf mergers ($\sim 0.3\%$) but also the coalescence of a
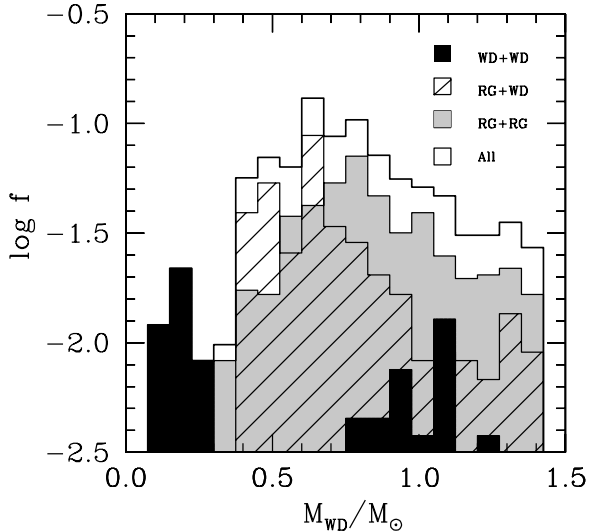
Figure 2. Mass distribution of the remnants of the mergers. The distribution shows the frequency of the different merger channels. The black histogram shows the masses of the remnants of the mergers of double white dwarf binaries, the dashed histogram of the mergers of a binary system composed of a red giant and a white dwarf, and the shaded histogram of the mergers of two red giants. The total mass distribution is shown using a solid line.

white dwarf and a giant star with a degenerate core ($\sim$1.1%) as well as the merger of two giants with degenerate cores ($\sim$1.5%). In these two last cases—namely, the merger of a white dwarf and a giant and the merger of two giant stars—the coalescences occur during the common envelope phase, while the merger of two white dwarfs is driven by gravitational wave radiation. Finally, we emphasize that the number of white dwarf mergers we obtain is in line with those obtained using completely different approaches (Bogomazov & Tutukov 2009)—see below for a detailed comparison with our results for the solar neighborhood—and that the distribution of remnant masses is nearly flat, in accordance with the observed distribution of masses of magnetic white dwarfs (Należyty & Madej 2004).

To better illustrate this last issue, Figure 2 shows the frequency distribution of remnant masses of the different merger channels for a sample of 10^3 mergers. We assumed that the remnant of each coalescence has a mass $M = M_1 + M_2/2$, where M_1 and M_2 stand, respectively, for the masses of the primary and secondary degenerate cores. This choice is in accordance with the results of the SPH simulations of Lorén-Aguilar et al. (2009), which show that approximately half of the secondary is accreted onto the primary, while the rest of the mass of the disrupted secondary forms a debris region and little mass is ejected during the merger. We also eliminated all those remnants that have masses larger than Chandrasekhar's limit, while, for the mergers producing a helium white dwarf, we adopted the procedure of Hurley et al. (2002). As can be seen, the total mass distribution (open histogram) presents a first peak for masses smaller than $\sim$0.4 $M_\odot$, corresponding to mergers in which a helium white dwarf is produced, then sharply increases for increasing remnant masses and, afterward, smoothly decreases for masses larger than $\sim$0.6 $M_\odot$. When this distribution is sampled for $\sim$26 objects with masses ranging from 0.8 $M_\odot$ to 1.4 $M_\odot$, we usually obtain fairly flat distributions, although the scarce number of objects and the subsequent large deviations prevent a sound comparison with the observational data.

Within 20 pc of the Sun there are 122 white dwarfs (Holberg et al. 2008), and several of them are magnetic (Kawka et al.

2007). This sample is 80% complete, but it is subject to poor statistics. However, it is useful because we have a reliable determination of the true incidence of magnetism in white dwarfs. Mass determinations are available for 121 of them. In the local sample, there are 14 magnetic white dwarfs, eight have magnetic fields in excess of 10^7 G, and three have masses larger than 0.8 $M_\odot$—a value which is $\sim$2.5σ away from the average mass of field white dwarfs. The selection of this mass cut is somewhat arbitrary, but, given the strong bias introduced by the initial mass function, we expect that the vast majority of high-field magnetic white dwarfs more massive than 0.8 $M_\odot$ would be the result of stellar mergers. This is indeed the case since our population synthesis calculations predict that about four white dwarfs are the result of double degenerate mergers and have masses larger than 0.8 $M_\odot$, which is in good agreement with observations. Additionally, our simulations predict that the fraction of white dwarfs more massive than $\sim$0.8 $M_\odot$ resulting from single stellar evolution is $\sim$10%. Consequently, the expected number of massive white dwarfs in the local sample should be $\sim$12. Instead, the local sample contains 20, pointing toward a considerable excess of massive white dwarfs, which could be the progeny of mergers. The rest of the population of magnetic white dwarfs (about five) would be the result of the evolution of single stars (Aznar Cuadrado et al. 2004). In this case, the magnetic field could have been generated during the red giant phase (Blackman et al. 2001), or it could be a fossil of the evolution of magnetic Ap or Bp stars—see, for instance, Mathys et al. (2001) and references therein. Nevertheless, it is worth noting that it has been recently suggested that these massive main-sequence stars are also the result of stellar mergers (Tutukov & Fedorova 2010).

The number of coalescing binaries previously discussed compares well with other results obtained using very different population synthesis codes. For instance, Bogomazov & Tutukov (2009), who used a completely independent code, obtained $\sim$7$\pm$1, where we have assumed Poissonian errors and white dwarf mergers within 20 pc of the Sun—see their Table 1—whereas we obtain $\sim$4$\pm$2. Thus, within the sampling uncertainties, both numbers qualitatively agree, despite the very small number of objects and the existing theoretical uncertainties, which include, among others, completely different approaches to simulate a representative sample of binaries, the ingredients necessary to model the Galaxy as a whole, and the parameters adopted in the calculation of the common envelope phase.

4. SUMMARY AND CONCLUSIONS

We have shown that the hot, convective, differentially rotating corona predicted by detailed three-dimensional simulations of the merger of two degenerate stellar cores can produce very high magnetic fields. We have also shown that these magnetic fields are confined to the outer layers of the remnant of the coalescence, and they propagate neither to the interior of the white dwarf nor to the debris region. Our model naturally predicts that high-field magnetic white dwarfs should preferentially have high masses, and they should be observed as single white dwarfs, as observationally found. Moreover, if the rotation and magnetic axes are not aligned, magnetodipole radiation rapidly spins down the magnetic white dwarf in short timescales. Thus, high-field magnetic white dwarfs may have a great variety of rotation periods. Moreover, in the case where the masses of the coalescing white dwarfs are not equal, the heavy, rotationally supported disk can survive for long periods of time, and a

planetary system could eventually form. The disruption of small planets could then contaminate the very outer layers of the magnetic white dwarf, explaining the recently discovered population of metallic magnetic white dwarfs. By contrast, if the masses of the merging white dwarfs are similar, the remnant has spherical symmetry and rotates very rapidly, as observed in some of the high-field magnetic white dwarfs. Also, the geometry of the surface magnetic fields can be well explained by our model. Finally, we have also shown that the expected number of double degenerate mergers is roughly consistent with the number of high-field magnetic white dwarfs in the local sample. In summary, our calculations indicate that a sizable fraction of all high-field magnetic white dwarfs could be the result of double degenerate mergers, which is in accordance with previous suggestions (Wickramasinghe & Ferrario 2000) not hitherto proven.

REFERENCES

Angel, J. R. P., Borra, E. F., & Landstreet, J. D. 1981, ApJS, 45, 457
Aznar Cuadrado, R., Jordan, S., Napiwotzki, R., et al. 2004, A&A, 423, 1081
Benacquista, M., Sedrakian, D. M., Hairapetyan, M. V., Shahabasyan, K. M., & Sadoyan, A. A. 2003, ApJ, 596, L223
Blackman, E. G., Frank, A., Markiel, J. A., Thomas, J. H., & Van Horn, H. M. 2001, Nature, 409, 485
Bogomazov, A. I., & Tutukov, A. V. 2009, Astron. Rep., 53, 214
Braithwaite, J. 2009, MNRAS, 397, 763
Cassisi, S., Potekhin, A. Y., Pietrinferni, A., Catelan, M., & Salaris, M. 2007, ApJ, 661, 1094
Clayton, G. C., Geballe, T. R., Herwig, F., Fryer, C., & Asplund, M. 2007, ApJ, 662, 1220
Dautray, R., & Lions, J. L. 2000, Mathematical Analysis and Numerical Methods for Science and Technology, Vol. 6 (Heidelberg: Springer)
Dewi, J. D. M., & Tauris, T. M. 2000, A&A, 360, 1043
Dupuis, J., Chayer, P., Vennes, S., Allard, N. F., & Hébrard, G. 2003, ApJ, 598, 486
Eggleton, P. P. 1983, ApJ, 268, 368
Euchner, F., Jordan, S., Beuermann, K., Reinsch, K., & Gänsicke, B. T. 2006, A&A, 451, 671
Euchner, F., Reinsch, K., Jordan, S., Beuermann, K., & Gänsicke, B. T. 2005, A&A, 442, 651
Farihi, J., Dufour, P., Napiwotzki, R., & Koester, D. 2011, MNRAS, 413, 2559
Ferrario, L., Vennes, S., Wickramasinghe, D. T., Bailey, J. A., & Christian, D. J. 1997, MNRAS, 292, 205
García-Berro, E., Lorén-Aguilar, P., Pedemonte, A. G., et al. 2007, ApJ, 661, L179
García-Berro, E., Torres, S., Isern, J., & Burkert, A. 1999, MNRAS, 302, 173
García-Berro, E., Torres, S., Isern, J., & Burkert, A. 2004, A&A, 418, 53
Guerrero, J., García-Berro, E., & Isern, J. 2004, A&A, 413, 257
Heggie, D. C. 1975, MNRAS, 173, 729
Holberg, J. B., Sion, E. M., Oswalt, T., et al. 2008, AJ, 135, 1225
Holmberg, J., & Flynn, C. 2000, MNRAS, 313, 209
Hurley, J. R., Pols, O. R., & Tout, C. A. 2000, MNRAS, 315, 543
Hurley, J. R., Tout, C. A., & Pols, O. R. 2002, MNRAS, 329, 897
Iben, I., Jr., & Tutukov, A. V. 1984, ApJS, 54, 335
Izzard, R. G., Jeffery, C. S., & Lattanzio, J. 2007, A&A, 470, 661
Jackson, J. D. 1998, Classical Electrodynamics (3rd ed.; New York: Wiley)
Kawka, A., & Vennes, S. 2011, A&A, 532, A7
Kawka, A., Vennes, S., Schmidt, G. D., Wickramasinghe, D. T., & Koch, R. 2007, ApJ, 654, 499
King, A. R., Pringle, J. E., & Wickramasinghe, D. T. 2001, MNRAS, 320, L45
Kroupa, P., Tout, C. A., & Gilmore, G. 1993, MNRAS, 262, 545
Kudritzki, R. P., & Reimers, D. 1978, A&A, 70, 227
Külebi, B., Jordan, S., Nelan, E., Bastian, U., & Altmann, M. 2010, A&A, 524, A36
Longland, R., Lorén-Aguilar, P., José, J., et al. 2011, ApJ, 737, L34
Lorén-Aguilar, P., Guerrero, J., Isern, J., Lobo, J. A., & García-Berro, E. 2005, MNRAS, 356, 627
Lorén-Aguilar, P., Isern, J., & García-Berro, E. 2009, A&A, 500, 1193
Mathys, G., Solanki, S. K., & Wickramasinghe, D. T. (ed.) 2001, in ASP Conf. Proc. 248, Magnetic Fields Across the Hertzsprung-Russell Diagram (San Francisco, CA: ASP)
Należyty, M., & Madej, J. 2004, A&A, 420, 507
Nelemans, G., Yungelson, L. R., Portegies Zwart, S. F., & Verbunt, F. 2001, A&A, 365, 491
Nordhaus, J., Wellons, S., Spiegel, D. S., Metzger, B. D., & Blackman, E. G. 2011, Proc. Natl. Acad. Sci., 108, 3135
Potter, A. T., & Tout, C. A. 2010, MNRAS, 402, 1072
Reimers, D., Jordan, S., & Christlieb, N. 2004, A&A, 414, 1105
Renedo, I., Althaus, L. G., Miller Bertolami, M. M., et al. 2010, ApJ, 717, 183
Schmidt, G. D., Bergeron, P., Liebert, J., & Saffer, R. A. 1992, ApJ, 394, 603
Schmidt, G. D., Harris, H. C., Liebert, J., et al. 2003, ApJ, 595, 1101
Schmidt, G. D., West, S. C., Liebert, J., Green, R. F., & Stockman, H. S. 1986, ApJ, 309, 218
Schreiber, M. R., & Gänsicke, B. T. 2003, A&A, 406, 305
Segretain, L., Chabrier, G., & Mochkovitch, R. 1997, ApJ, 481, 355
Silvestri, N. M., Lemagie, M. P., Hawley, S. L., et al. 2007, AJ, 134, 741
Spitkovsky, A. 2006, ApJ, 648, L51
Tayler, R. J. 1973, MNRAS, 161, 365
Timokhin, A. N. 2006, MNRAS, 368, 1055
Torres, S., García-Berro, E., Burkert, A., & Isern, J. 2002, MNRAS, 336, 971
Tout, C. A., Wickramasinghe, D. T., Liebert, J., Ferrario, L., & Pringle, J. E. 2008, MNRAS, 387, 897
Tutukov, A. V., & Fedorova, A. V. 2010, Astron. Rep., 54, 156
Valyavin, G., & Fabrika, S. 1999, in ASP Conf. Proc. 169, Proc. of the 11th European Workshop on White Dwarfs, ed. S. E. Solheim & E. G. Meistas (San Francisco, CA: ASP), 206
Vassiliadis, E., & Wood, P. R. 1993, ApJ, 413, 641
Webbink, R. F. 1984, ApJ, 277, 355
Wendell, C. E., van Horn, H. M., & Sargent, D. 1987, ApJ, 313, 284
Wickramasinghe, D. T., & Ferrario, L. 2000, PASP, 112, 873
Yoon, S.-C., Podsiadlowski, P., & Rosswog, S. 2007, MNRAS, 380, 933
Zorotovic, M., Schreiber, M. R., Gänsicke, B. T., & Nebot Gómez-Morán, A. 2010, A&A, 520, A86